frontiers in Earth Science

ORIGINAL RESEARCH
published: 30 August 2019
doi: 10.3389/feart.2019.00217

Partitioning Pervasive Detrital Geochronologic Age Distributions in the Southern Alaskan Forearc

*Emily S. Finzel**

Department of Earth and Environmental Sciences, University of Iowa, Iowa City, IA, United States

The extensive detrital zircon U-Pb geochronologic dataset presented here includes new and compiled data (*N* = 38; *n* = 8,006) from modern rivers that together comprehensively characterizes the geographic distribution of pervasive Mesozoic—Cenozoic igneous belts across mountainous regions in south-central Alaska, including the northern Chugach Mountains, Talkeetna Mountains, and western, central, and eastern Alaska Range. These data are compared to an extensive detrital zircon U-Pb dataset from Lower Cretaceous to Pliocene strata in the forearc basin (*N* = 29; *n* = 8,678) using a recently developed unmixing approach to investigate the variations in long-term provenance and sediment dispersal patterns in the basin in response to tectonic events. During the Early Cretaceous, the primary sediment source was an exhumed Jurassic arc located north of the basin, but new sediment derived from accretionary prism strata in the northern Chugach Mountains during the Late Cretaceous coincides with final suturing of the Insular terranes with North America and a change in plate kinematics. Eocene strata record major sediment derivation from the western Alaska Range after passage of a subducting spreading ridge. By the Oligocene, shallow subduction of the Yakutat microplate triggered a rejuvenation of exhumation in the northern Chugach Mountains that continued through the Early-Middle Miocene. And overall inboard shift of dominant source regions to the Talkeetna Mountains and central Alaska Range likely reflects the continued insertion of the shallow slab beneath south-central Alaska. The integrated approach of strategic modern river sampling and comprehensive basin strata characterization in conjunction with an inverse Monte Carlo approach of mixture modeling demonstrates a useful approach for partitioning of widespread and pervasive ages in sediment source terranes.

Keywords: detrital zircon, U-Pb geochronology, forearc basin, Alaska, mixture modeling

OPEN ACCESS

Edited by:
Miquel Poyatos Moré, University of Oslo, Norway

Reviewed by:
Daniel Stephen Coutts, University of Calgary, Canada
Andrea Stevens Goddard, Rowan University, United States
Jeffrey M. Amato, New Mexico State University, United States

***Correspondence:**
Emily S. Finzel
emily-finzel@uiowa.edu

Specialty section:
This article was submitted to Sedimentology, Stratigraphy and Diagenesis, a section of the journal Frontiers in Earth Science

***Received:** 26 April 2019*
***Accepted:** 09 August 2019*
***Published:** 30 August 2019*

Citation:
Finzel ES (2019) Partitioning Pervasive Detrital Geochronologic Age Distributions in the Southern Alaskan Forearc. Front. Earth Sci. 7:217. doi: 10.3389/feart.2019.00217

INTRODUCTION

Detrital zircon U-Pb geochronology of sandstone is routinely used for determining provenance and sediment dispersal patterns in basins, maximum depositional age of clastic strata, and magmatic and exhumational histories of sediment source regions (DeCelles et al., 1998; DeGraaff-Surpless et al., 2002; Fedo et al., 2003; Weislogel et al., 2006; Gehrels et al., 2008; Dickinson and Gehrels, 2009). For provenance, the usefulness of single-grain U-Pb dating of zircons in any specific area is contingent upon knowing the ages of zircons in all potential source regions, as well as having a distribution of unique ages among the igneous sources. In many regions with prolonged magmatic histories, however, individual igneous belts can be geographically extensive and plutonic belts of different ages often overlap, making precise provenance determination difficult.

In south-central Alaska, widespread Middle to Late Jurassic magmatism was succeeded by profuse Late Cretaceous to early Eocene magmatism, followed by minor pulses of late Eocene-Oligocene magmatism. Detrital zircon grains with all these ages are abundant in the Late Mesozoic-Cenozoic forearc basin strata and compose ∼90% of the detrital age groups on average. Even so, these ages groups were previously difficult to interpret given the widespread nature of the source rocks and lack of extensive bedrock dating in the source regions. The new and compiled data presented here represents the first comprehensive geographic characterization of these igneous sources via U-Pb dating of detrital zircons from modern rivers (N = 38; n = 8,006) in the northern Chugach Mountains, Talkeetna Mountains, and western, central, and eastern Alaska Range. These data, in conjunction with an extensive detrital zircon U-Pb dataset from Lower Cretaceous to Pliocene strata in the forearc basin (N = 29; n = 8,678), are evaluated using a recently developed unmixing approach (Sundell and Saylor, 2017) to more fully resolve the long-term provenance and sediment dispersal patterns in the basin. Although not the goal of this paper, the resulting temporal variations in source areas and sediment dispersal patterns are interpreted to be related to several significant tectonic events in south-central Alaska, including Late Cretaceous accretion of the Insular terranes, Paleocene to Eocene migration of a subducting spreading ridge, and on-going shallow subduction of an oceanic plateau since Oligocene time. The main focus of this paper is to demonstrate that the combined approach of extensive and strategic modern river sampling to resolve age groups in potential sediment source areas and comprehensive characterization of detrital age groups in basin strata in conjunction with mixture modeling offers the ability to partition between widespread and pervasive ages in sediment source terranes.

EXISTING PROVENANCE AND TECTONIC MODELS

Convergence and subduction have been continuous along the outboard margin of south-central Alaska since at least Jurassic time, accompanied by several different subduction-related events, including terrane accretion, spreading-ridge subduction, and flat-slab subduction of an oceanic plateau. During Middle Jurassic to Late Cretaceous time, the Insular terranes, upon which the forearc basin and study areas are situated, collided with the outboard margin of western North America (Pavlis, 1982; McClelland et al., 1992; Trop et al., 2002, 2005; Manuszak et al., 2007); subduction along the outboard margin of the terranes continued during Late Cretaceous time (Plafker et al., 1994; Trop and Ridgway, 2007).

Mesozoic sedimentary and volcanic forearc basin strata are exposed along the southern margin of the Talkeetna Mountains in south-central Alaska (**Figure 1**). There, two lower Cretaceous sedimentary units have received very little attention and are simply mapped as the Ks unit (Cretaceous sandstone) and Kc unit (Cretaceous calcareous sandstone) in the Talkeetna Mountains (Grantz, 1960). Detrital zircon U-Pb geochronologic data and $\varepsilon Hf_{(t)}$ values from those units are interpreted to record increased erosional exhumation of the adjacent Jurassic arc and access to deeper and older parts of the batholith, as well as initial input of sediment from local Paleozoic basement sources (Reid et al., 2018).

Lying unconformably above the Lower Cretaceous strata is the Upper Cretaceous Matanuska Formation. Early work based on sandstone petrography, zircon U-Pb ages of granitic clasts, and sparse detrital zircon U-Pb ages inferred that the provenance of the upper Matanuska Formation was Jurassic–Cretaceous igneous rocks located north of the basin (Trop, 2008). More recently, Reid et al. (2018) presented new detrital zircon U-Pb data as well as $\varepsilon Hf_{(t)}$ values that also suggest sediment derivation from the proximal Jurassic and Late Cretaceous arc rocks as well as initial influx of sediment from older inboard terranes.

During Paleocene and Eocene time (ca. 62–50 Ma), either a spreading ridge that subducted from west to east across the entire southern margin, or a slab break-off event following final suturing of the Insular terranes, resulted in a hiatus in arc magmatism, emplacement of slab-window igneous rocks in the forearc and accretionary prism regions, and high-temperature/low-pressure metamorphism of accretionary prism strata (Bradley et al., 2003; Haeussler et al., 2003; Sisson et al., 2003; Cole et al., 2006; Terhune et al., 2019; Trop et al., 2019). In addition, previous detrital geochronologic and thermochronologic data from the Alaskan forearc basin demonstrate that after this event retro-arc sources become predominant over more proximal arc sources (Finzel et al., 2016).

Either subduction of oceanic crust with normal slab dip or a period of transform tectonics following slab break-off briefly occurred after spreading-ridge subduction until the late Eocene or early Oligocene (∼35 Ma) when subduction of the Yakutat microplate initiated shallow subduction along the outboard margin of south-central Alaska and continues to the present day (Finzel et al., 2011, 2015; Arkle et al., 2013; Terhune et al., 2019; Trop et al., 2019). The Yakutat microplate is an ∼11–30 km thick, wedge-shaped oceanic plateau that is subducting at a dip angle of 11–16°, decreasing from west to east, to near the modern coastline (Ferris et al., 2003; Eberhart-Phillips et al., 2006; Worthington et al., 2008, 2012; Christeson et al., 2010; Bauer et al., 2014). Yakutat shallow-subduction-related processes observed in the upper plate in Alaska include changes in (1) the style and location of volcanic arc magmatism, (2) sedimentary basin subsidence and inversion patterns, and (3) sediment sources as a result of accelerated surface uplift above the subducted flat slab (e.g., Enkelmann et al., 2008, 2019; Finzel et al., 2011, 2015, 2016; Trop et al., 2012; Arkle et al., 2013; Finzel and Enkelmann, 2017). Shallow subduction still characterizes the present-day margin of southern Alaska.

Cenozoic strata in the Cook Inlet forearc basin crop out in discontinuous belts along the margins of the basin and depositionally overlie or are in fault contact with rocks of the adjacent accretionary prism and volcanic arc

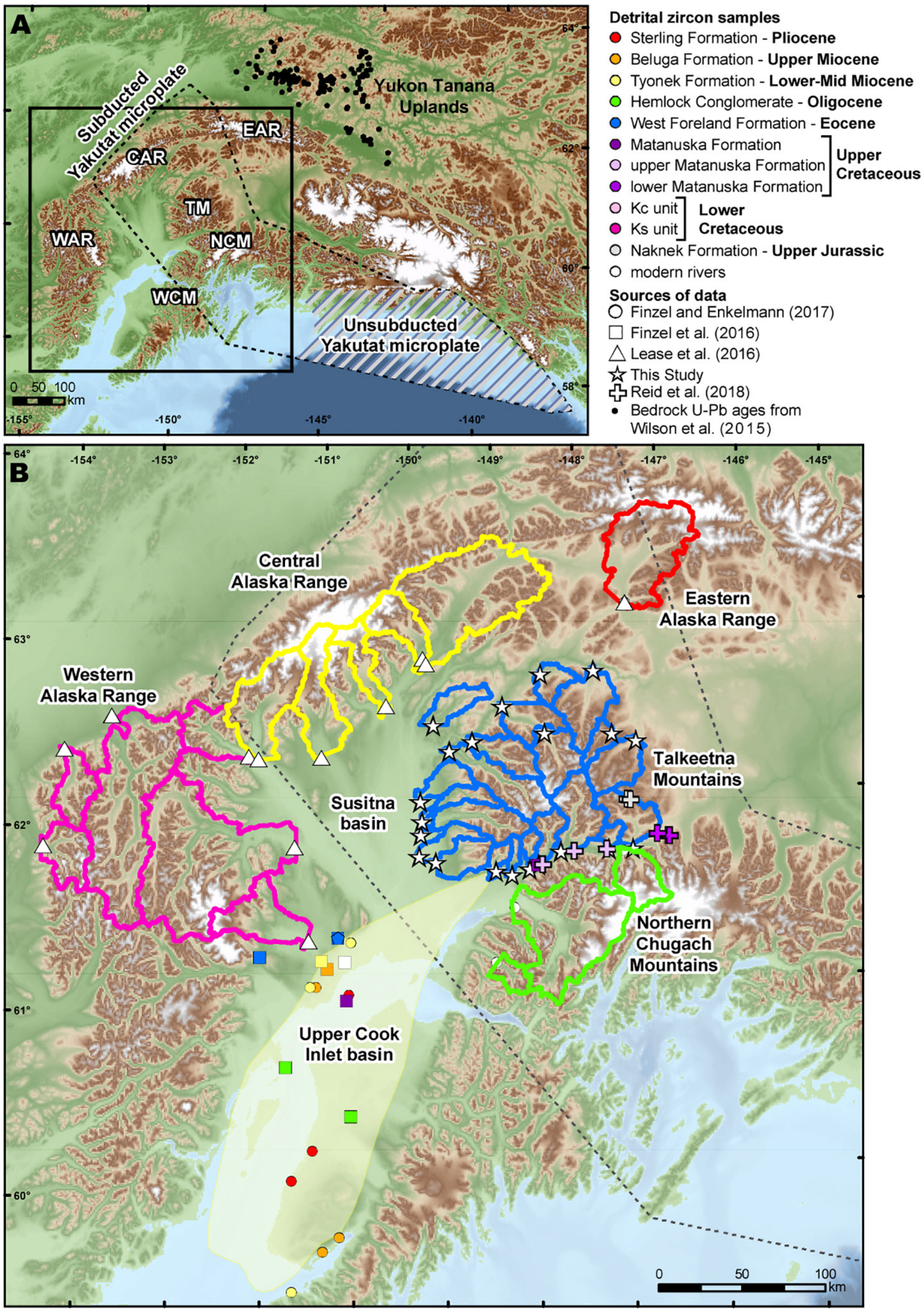

FIGURE 1 | (A) Location map of south-central Alaska showing extent of subducted and unsubducted Yakutat microplate, major mountain belts, the Yukon Tanana Uplands, and the study area (black box is area shown in **(B)**. WAR, western Alaska Range; CAR, central Alaska Range; EAR, eastern Alaska Range; TM, Talkeetna Mountains; NCM, northern Chugach Mountains; WCM, western Chugach Mountains. **(B)** Location map of the study area showing the watersheds for detrital zircon samples from modern rivers in the western Alaska Range (pink), central Alaska Range (yellow), eastern Alaska Range (red), Talkeetna Mountains (blue), and northern Chugach Mountains (green), locations of basin strata samples, and generalized outline of the modern-day Cook Inlet basin. Note that forearc strata are contained within the basin, whereas accretionary prism strata are found in the uplifted Chugach Mountains. The sample symbols denote both the source of the data (by shape) and the depositional age (by color).

(Magoon et al., 1976). In the center of the basin, the forearc strata unconformably overlie Mesozoic sedimentary and volcanic rocks (Jones and Silberling, 1979; Magoon and Egbert, 1986). The upper Paleocene to early Eocene West Foreland Formation reaches its maximum thickness along the western margin of the basin and thins toward the center of the basin (Calderwood and Fackler, 1972; Kirschner and Lyon, 1973; Houston, 1994; Swenson, 1997). The Oligocene Hemlock Conglomerate forms a sheet that is ~200–845 m thick across most of the basin (Magoon et al., 1976; Wolfe and Tanai, 1980; Flores et al., 2004). These units postdate spreading-ridge subduction and record the response to this event as an expansion of forearc depositional systems during middle Eocene to late Oligocene time (Finzel et al., 2015, 2016). Detrital zircon U-Pb and $\varepsilon Hf_{(t)}$ signatures reflect both a continuation of local arc-region-derived sediment and also a significant change to distal retro-arc region sediment sources, including the Yukon-Tanana Uplands (**Figure 1**).

Stratigraphic units that are dominantly Neogene in age were deposited in the basin as flat-slab subduction of the Yakutat slab was underway to the northeast (Finzel et al., 2011). The upper Oligocene to middle Miocene Tyonek Formation averages approximately 2,400 m thick across the entire basin (Wolfe and Tanai, 1980). The middle to upper Miocene Beluga Formation reaches its maximum thickness of ~1,800 m near the western margin of the basin and thins to the east where it is truncated by the overlying Sterling Formation (Calderwood and Fackler, 1972; Kirschner and Lyon, 1973). The upper Miocene to Pliocene Sterling Formation is the only Cenozoic formation in the basin that is thickest near the eastern margin, where it is ~3,300 m thick (Calderwood and Fackler, 1972; Kirschner and Lyon, 1973). Detrital zircon U-Pb and $\varepsilon Hf_{(t)}$ signatures in these strata record the shrinking of basin catchments and a shift toward more local sediment sources in the adjacent arc rocks in response to insertion of the shallow Yakutat slab (Finzel et al., 2016; Finzel and Enkelmann, 2017).

U-Pb GEOCHRONOLOGY DATA

This study focuses on the potential sources of Mesozoic and younger detrital zircon grains in the forearc strata, and therefore only ages younger than 250 Ma were used in the models. Source regions were characterized by detrital zircon U-Pb ages primarily from modern rivers, except for the Yukon Tanana Uplands that is characterized by bedrock data (**Figure 1**, **Table 1**, and **Supplementary Data Sheet S1**). Sampling of rivers provides a much more comprehensive view of all igneous ages present in a watershed when compared to bedrock sampling, which is often focused on individual igneous bodies or groups of bodies, or on solving a precise temporal problem. New samples from twenty rivers within the Talkeetna Mountains are presented here and fully characterize the bedrock of the entire mountain range with n_{total} = 5,820 and $n_{<250\ Ma}$ = 5,656 (**Figure 2**). Twenty sandstone samples were collected from rivers that drain the Talkeetna Mountains. Samples were processed using standard mineral separation techniques at the University of Iowa to extract a heavy mineral separate. The separate was sieved using disposable 350 μm screen and non-zircon was removed by magnetic and density separations. A random aliquot was handpicked under alcohol to remove all non-zircon, resulting in a final separate of approximately 500 grains for each sample. Mounts were made at the University of Iowa. Detrital zircons were analyzed for U-Pb isotopes by laser-ablation-multicollector-inductively coupled plasma-mass spectrometry (LA-MC-ICPMS) at the Arizona LaserChron Center following the methods of Gehrels et al. (2006) and Gehrels (2012). The majority of the analyses were conducted with a laser spot diameter of 20 μm. Approximately 315 detrital zircon grains from each sample were analyzed. The $^{206}Pb/^{238}U$ ages are presented for all grains. The U-Pb analytical data is reported in the **Supplementary Data Sheet S1**.

The detrital signature of the western Alaska Range is determined from seven previously published samples with n_{total} = 419 and $n_{<250\ Ma}$ = 397 (Finzel et al., 2016; Lease et al., 2016). Five samples from rivers draining the southern flank of the central Alaska Range have n_{total} = 487 and $n_{<250\ Ma}$ = 463 (Lease et al., 2016). The eastern Alaska Range is the least well-characterized with only two samples that produce with n_{total} = 186 and $n_{<250\ Ma}$ = 184 (Lease et al., 2016; Finzel and Enkelmann, 2017). To the south, the detrital signature of Permian-Cretaceous accretionary prism strata in the northern Chugach Mountains is represented by three samples with n_{total} = 969 and $n_{<250\ Ma}$ = 914 (Finzel and Enkelmann, 2017). No modern river data was available for the Yukon Tanana Uplands located northeast of the eastern Alaska Range (**Figure 1**), but that region was previously identified as an important sediment source area during the early Cenozoic based on Paleozoic and Precambrian ages present in the basin strata (Finzel et al., 2016). Therefore, 125 previously published monazite, sphene, titanite, and zircon U-Pb ages from bedrock were combined and are here treated as a detrital signature for the area.

Forearc basin strata were subdivided into individual or groups of formations that represent seven different time intervals (**Table 2**). Three samples from the Kc and Ks units from the Talkeetna Mountains (**Figure 1**) embody Early Cretaceous time with n_{total} = 1,081 and $n_{<250\ Ma}$ = 1,051. The Late Cretaceous is represented by eight samples from the Matanuska Formation that have n_{total} = 2,550 and $n_{<250\ Ma}$ = 2,314. Three samples from the West Foreland Formation characterize the Eocene

TABLE 1 | Data information for sediment source regions.

Geographic region	Sources of data	*N* =	n_{total} =	$N_{<250\ Ma}$ =	$\%_{<250Ma}$
Talkeetna Mountains	This study	21	5820	5656	97%
Western Alaska Range	Finzel et al., 2016; Lease et al., 2016	7	419	397	95%
Central Alaska Range	Lease et al., 2016	5	487	463	95%
Eastern Alaska Range	Lease et al., 2016; Finzel and Enkelmann, 2017	2	186	184	99%
Chugach Mountains	Finzel and Enkelmann, 2017	3	969	914	94%
Yukon Tanana Uplands*	Wilson et al., 2015	125	125	125	100%

**Data from bedrock samples were filtered for <250 Ma.*

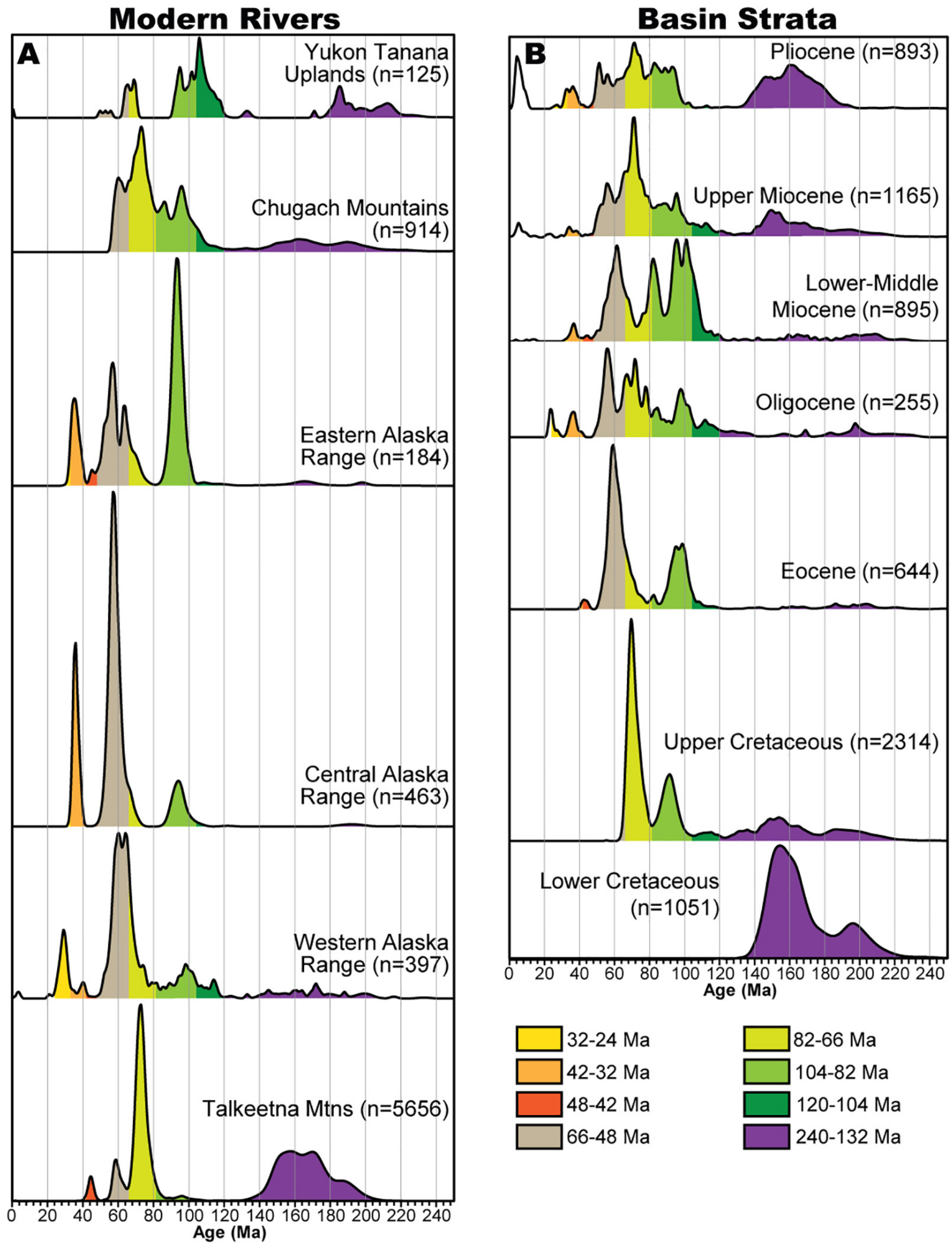

FIGURE 2 | Probability density plots of geochronological data from **(A)** potential source regions and **(B)** forearc basinal strata.

TABLE 2 | Data and model information for each stratigraphic interval.

Stratigraphic interval	Sources of data	N =	n_{total} =	n = $_{<250\ Ma}$	$\%_{<250\ Ma}$	Min. age	R^2
Pliocene	Finzel and Enkelmann, 2017	3	916	893	97%	20 Ma	0.697
Upper Miocene	Finzel et al., 2016; Finzel and Enkelmann, 2017	4	1248	1165	93%	20 Ma	0.931
Lower-Middle Miocene	Finzel et al., 2016; Finzel and Enkelmann, 2017	4	1023	895	87%	20 Ma	0.691
Oligocene	Finzel et al., 2016	2	342	255	75%	23 Ma	0.833
Eocene	Finzel et al., 2016; Enkelmann et al., 2019	3	900	644	72%	40 Ma	0.902
Upper Cretaceous	Finzel et al., 2016; Reid et al., 2018	8	2550	2314	91%	65 Ma	0.895
Lower Cretaceous	Reid et al., 2018	3	1081	1051	97%	84 Ma	0.856

with n_{total} = 900 and $n_{<250\ Ma}$ = 644. The Oligocene is epitomized by two samples from the Hemlock Formation that have n_{total} = 342 and $n_{<250\ Ma}$ = 255. Four samples from the Tyonek Formation represent the Early-Middle Miocene with n_{total} = 1,023 and $n_{<250\ Ma}$ = 895. The Late Miocene is represented by four samples from the Beluga Formation with n_{total} = 1,248 and $n_{<250\ Ma}$ = 1,165. Three samples from the Sterling Formation characterize Pliocene time and have n_{total} = 916 and $n_{<250\ Ma}$ = 893.

Some of the samples used in this study are n = 100, and recent work has suggested that small-n detrital zircon studies may not be reliable for comparisons of relative proportions of populations between samples (Gehrels, 2012; Pullen et al., 2014). Finzel et al. (2016) compared a small-n data set first published in Finzel et al. (2015) with an expanded large-n (n = 300) data set and illustrated that they do not show a significant difference in the presence of major populations, as well as most minor populations. The similarity between the two sets of analyses is likely due to the small number of age groups in each sample. For example, as in this study, most of the distributions have two or three main peaks, so a smaller number of analyses were sufficient to characterize the distribution both in terms of the presence and relative abundance of age groups. Therefore, in basins with sources that have fewer age populations from which to derive sediment, smaller-n datasets may suffice for drawing comparisons.

MODELING APPROACH

The mixing proportions of the various source regions for each of the defined stratigraphic intervals were modeled using an inverse Monte Carlo approach in combination with an optimized forward model (DZMix from Sundell and Saylor, 2017). Details about the modeling procedure can be found in Sundell and Saylor (2017). In general, the inverse model consisted of 10,000 iterations where each source region's entire probability density plot (PDP) and kernel density estimate (KDE) were scaled by randomly generated weights and then summed together to produce a single model source distribution. While the maximum age modeled for each stratigraphic interval was 250 Ma, the minimum modeled age was dependent upon the known depositional age of the formation(s) or was designated 20 Ma because previous work has demonstrated that igneous rocks younger than that are not found in any abundance in the modeled source regions (**Table 2**; Finzel et al., 2011, 2015). For each stratigraphic interval, the 1% best-fit Monte Carlo trials are shown in **Figures 3–9**, along with the mean cross-correlation coefficient (R^2). This statistical parameter has been suggested to be more discriminating than other tests (e.g., KS and Kuiper) as well as more sensitive to the overall number and proportions of ages in a distribution (Sundell and Saylor, 2017). The best-fits from the inverse model are then forward modeled to minimize 1-R^2. This is shown as the optimized best-fit model and its associated R^2 in **Figures 3–9**. In addition, CDFs from the source areas and composite stratigraphic interval, as well as the resultant relative contributions from each source region based on the optimized forward model, are displayed.

MODEL RESULTS

Model results for Lower Cretaceous strata suggest that the predominant sediment source region, with more than 90% of the zircon signature being derived, was in the Talkeetna Mountains (**Figure 3**). The R^2 for the optimized best-fit model is 0.856. The small misfit probably results from the model's inability to parse out and differentially weight individual age groups from the source signatures. That is, the weighting factor is applied

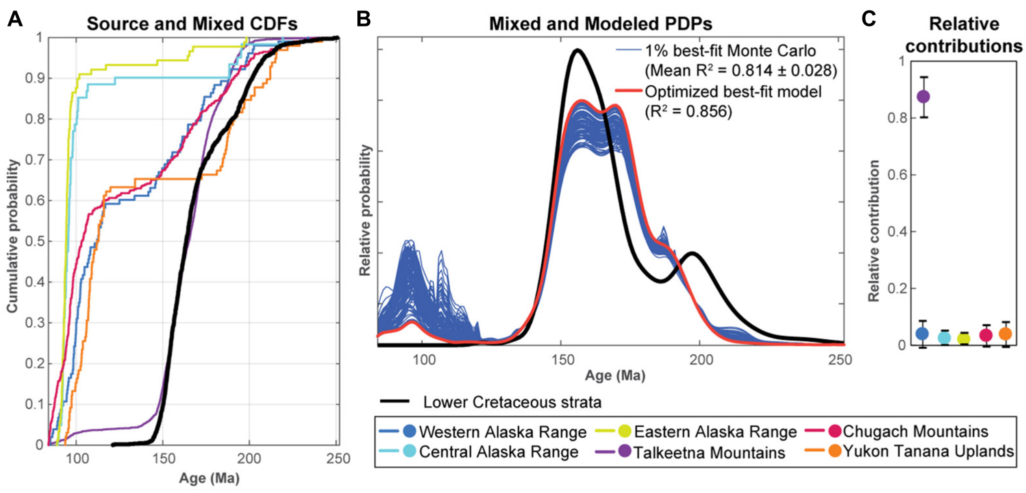

FIGURE 3 | Model results for Lower Cretaceous strata showing **(A)** cumulative density functions for the basin strata and potential source regions, **(B)** probability density plots of the basin strata (black), 1% best-fits from the Monte Carlo inverse model (blue), and optimized best-fit forward model (red), and **(C)** plot of relative contributions from each of the potential source regions produced from the optimized best-fit model.

to the entire age distribution, such that in this example, the model has to include some Cretaceous ages that are found in the Talkeetna Mountains today but do not appear in the zircon signature of the Lower Cretaceous strata. These results suggest a more localized source for the strata that is characterized solely by Jurassic zircon sources.

In contrast, sediment source regions for Upper Cretaceous strata include approximately equal contributions from the Talkeetna Mountains and the accretionary prism strata in the northern Chugach Mountains (**Figure 4**). The R^2 for the optimized best-fit model is 0.895. The small misfit here is due to the underfitting of the 74 Ma peak in the Upper Cretaceous signature. This could be remedied by scaling the individual age peaks within the source contributions, and therefore does not require another sediment source region to improve the fit.

By the Eocene, sediment sources for the basin had changed significantly with negligible contributions from the previously important Talkeetna Mountains and northern Chugach Mountains. In contrast, model results for Eocene strata suggest the primary source region was in the western Alaska Range (**Figure 5**). The R^2 for the optimized best-fit model is 0.902. Overall, all of the individual age peaks found in the Eocene strata are matched by a western Alaska Range source, so the very small misfit is attributable to the underfitting of age peaks as before, specifically ∼61 and 100 Ma.

A second shift in sediment sources for the forearc basin occurred by the Oligocene. Model results for Oligocene strata indicate the primary sediment source region as the northern Chugach Mountains (∼40%), with lesser contributions from the central Alaska Range (∼20%), and minor contributions from the remaining source regions (**Figure 6**). The R^2 for the optimized best-fit model is 0.833. The primary source of the small misfit can be attributed to a ∼26 Ma peak in the Oligocene strata that is not matched by the model results. The source for these zircons has previously been identified as intrusive rocks found in the eastern Alaska Range region, but lies outside of our modern river data coverage (Turner and Smith, 1974; Nokleberg et al., 1992).

Model results for Lower—Middle Miocene strata have the lowest R^2 of any stratigraphic interval at 0.691 for the optimized best-fit model. Regardless, the results suggest a variety of sediment source regions, including the northern Chugach Mountains and Yukon Tanana Uplands (∼30% each) and western and eastern Alaska Ranges (∼15% each; **Figure 7**). The moderate misfit is clearly due to the model underfitting peaks ∼83 and 102 Ma, and overfitting peaks ∼180–190 Ma. An ∼83 Ma peak is not present in the source data, although the northern Chugach Mountains signature contains a peak ∼85 Ma, suggesting that not all the potential sources for the basin have been included in the source dataset. Underfitting of the ∼102 Ma peak and overfitting of the Jurassic peaks is the result of not weighting individual age peaks in the source distributions differently. The Yukon Tanana Uplands signature provides both of these age groups, but in different relative proportions than in the Lower—Middle Miocene strata. The model's attempt to fit the relatively large ∼102 Ma peak in the basin strata results in an overestimation of the Jurassic ages.

The R^2 for the optimized best-fit model of Upper Miocene strata is the highest for any stratigraphic interval at 0.931. The primary sediment source regions lie above the present-day flat slab region (**Figure 1**) and include the northern Chugach Mountains (∼60%) and the Talkeetna Mountains (∼30%; **Figure 8**). The optimized best-fit model matches not only the age peaks present, but also the relative abundances for each age peak very closely.

Model results for Pliocene strata have the second lowest R^2 of any stratigraphic interval at 0.697 for the optimized best-fit model. The primary sediment source region is the Talkeetna Mountains (∼60%), with a smaller contribution from the eastern Alaska Range (∼20%) and northern Chugach Mountains (∼10%; **Figure 9**). The moderate misfit is again attributable to underfitting a peak ∼85 Ma, but also overfitting a peak ∼74 Ma and underfitting Jurassic peaks between ∼165-150 Ma. The latter misfits are related because in the model's attempt to fit the abundant Jurassic ages found in the Pliocene strata and sourced from the Talkeetna Mountains, it must also input a significant proportion of ∼74 Ma ages also found in that source region. These results suggest a more localized source for the Pliocene strata in the Talkeetna Mountains that is characterized by dominantly Jurassic zircon sources with relatively less Late Cretaceous ages.

SEDIMENT DISPERSAL AND TECTONICS

Early Cretaceous

During Late Jurassic and Early Cretaceous time, regional exhumation of the Jurassic oceanic island arc north of the forearc basin was related to either collision of the arc with the other Insular terranes outboard of the North American margin (Clift et al., 2005) or collision of the entire Insular belt terranes, including the Jurassic arc, with the North American margin itself (Nokleberg et al., 2001; Ridgway et al., 2002; Trop et al., 2002, 2005; Blodgett and Sralla, 2008; Bacon et al., 2012). Basins positioned along the inboard margin of the Insular terranes and the outboard margin of North America contain evidence for initial Late Jurassic collision and Aptian to Campanian final suturing (Nokleberg et al., 1992; Ridgway et al., 1997, 2002; Eastham and Ridgway, 2002; Trop et al., 2004; Davidson and McPhillips, 2007; Hampton et al., 2007; Kalbas et al., 2007; Manuszak et al., 2007).

Detrital zircon U-Pb geochronologic data and $\varepsilon Hf_{(t)}$ values from the Lower Cretaceous strata were previously interpreted to record exhumation of deeper and older parts of the adjacent Jurassic arc and input from local Paleozoic basement sources that are part of the Insular terranes (Reid et al., 2018). The bedrock in the Talkeetna Mountains is mostly composed of Peninsular terrane rocks, which was originally defined by Jones et al. (1977), Jones and Silberling (1979), and Plafker et al. (1989) to consist of late Paleozoic carbonate and volcanics, Late Triassic carbonate and basalt, Late Triassic–Late Jurassic ultramafic, andesitic, and granitic rocks, and Middle Jurassic–Cretaceous clastic basinal

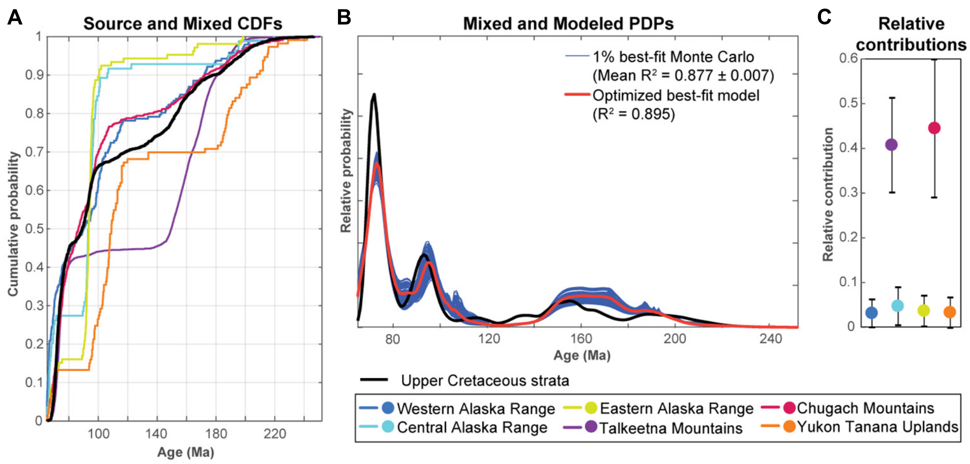

FIGURE 4 | Same as **Figure 3** except for the Upper Cretaceous strata.

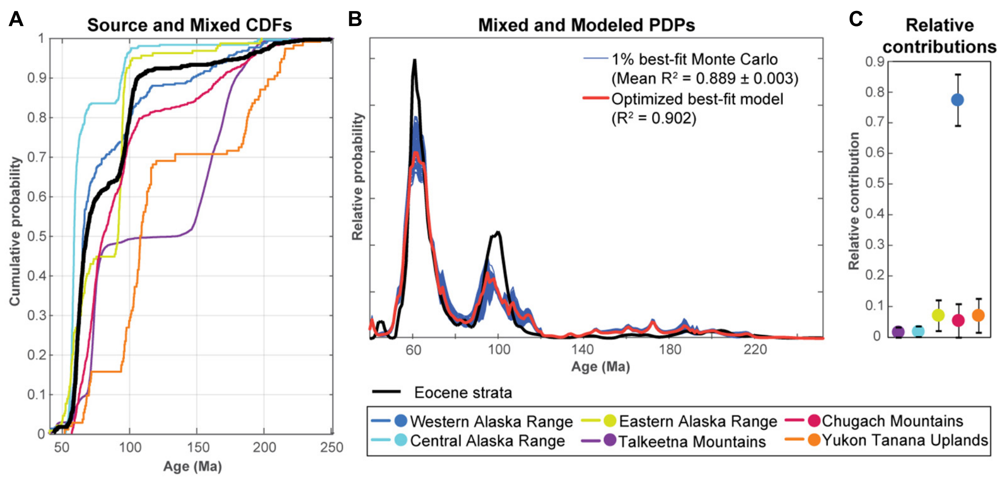

FIGURE 5 | Same as **Figure 3** except for the Eocene strata.

sequences. Recent work on the terrane has focused on the Early–Late Jurassic magmatic rocks of the Talkeetna oceanic island arc, and geochronologic bedrock data from the Talkeenta Mountains indicates magmatic activity between 202–181 Ma and 177–156 Ma, respectively (Rioux et al., 2007, 2010). The modeling results presented here support the previously inferred primary sediment source of the Talkeetna Mountains for grains younger than 250 Ma, and specifically a source characterized by Jurassic ages and less so by the older Insular basement rocks (**Figures 3**, **10**).

Late Cretaceous

By the Late Cretaceous, the Insular terranes were fully accreted to the North American margin, either at low paleolatitudes, near present-day Baja California, and then transported >3,000 km northward through strike-slip translation to its present-day position between Late Cretaceous and Paleocene time (Irving et al., 1985; Panuska, 1985; Umhoefer, 1987; Cowan et al., 1997; Stamatakos et al., 2001), or within ∼1,000 km of its present day position and subsequently transported northward over the same period (e.g., Irving et al., 1996; Butler et al., 1997; Keppie and Dostal, 2001). Detrital zircon U-Pb distributions and $\varepsilon Hf_{(t)}$ values in the Upper Cretaceous strata have pronounced Late Cretaceous peaks, diminished Jurassic grains, more abundant Paleozoic and Precambrian populations, and a wide range of negative $\varepsilon Hf_{(t)}$ values that signify an influx of sediment from the inboard Intermontane terranes to the forearc basin (Reid et al., 2018). That study also presented our preferred model where the forearc basin in south-central Alaska, the part of the Intermontane terranes that are today located in northern British Columbia, Yukon, and eastern Alaska, and the part of the Chugach-Prince William terrane found on Kodiak Island were all juxtaposed by Late Cretaceous (Turonian) time. Therefore, offset between the forearc basin and the potential sediment sources used in this study were not significant.

Modeling results for grains with ages <250 Ma in the Upper Cretaceous strata suggest an additional, previously undetected

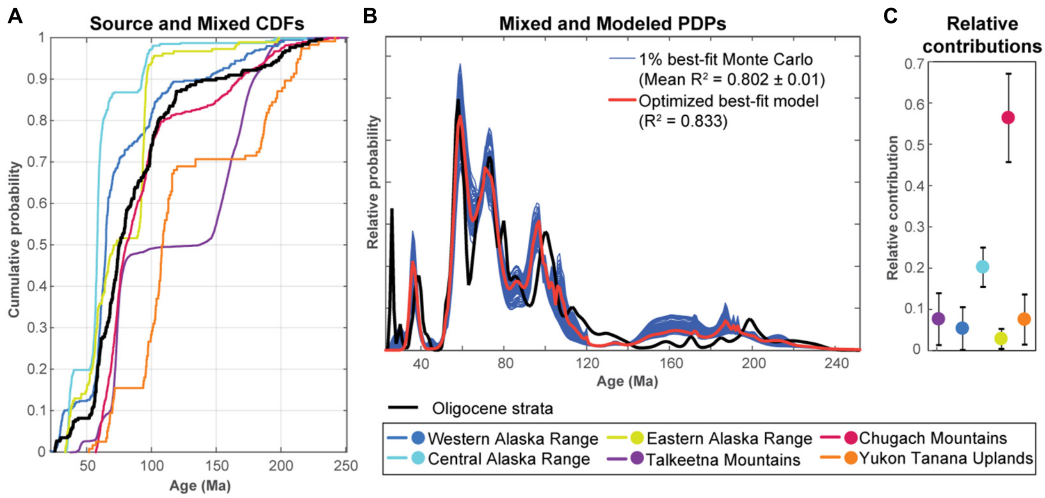

FIGURE 6 | Same as **Figure 3** except for the Oligocene strata.

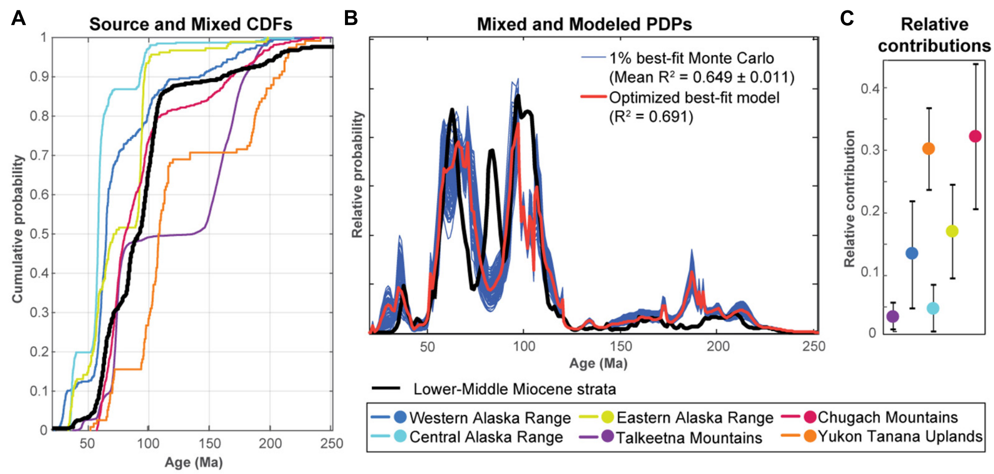

FIGURE 7 | Same as **Figure 3** except for the Lower-Middle Miocene strata.

source in the accretionary prism strata of the northern Chugach Mountains (**Figures 4, 10**). Coarse-grained sedimentation along the southern margin of the forearc basin contains diagnostic lithologies that imply local subaerial uplift and erosion of the accretionary prism by Early Cretaceous time (Trop and Ridgway, 2007). The results presented here indicate that Insular terrane rocks in the Talkeetna Mountains and accretionary prism strata in the northern Chugach Mountains contributed relatively equally to the zircon signature found in the Upper Cretaceous strata. This implies that the accretionary prism strata may have been extensively subaerially exhumed and eroding into the forearc basin during the Late Cretaceous.

Eocene

During Paleocene and Eocene time (~62–50 Ma), a spreading ridge was subducted while migrating from west to east across the entire southern Alaska margin. Deposition of middle Eocene (~44–41 Ma) strata postdates passage of the spreading ridge through the study area. Detrital zircon U-Pb and $\varepsilon Hf_{(t)}$ signatures from Eocene strata were previously interpreted to reflect a continuation of local arc region-derived sediment from the western and central Alaska Range and Talkeetna Mountains, based on Mesozoic and Cenozoic ages. In addition, a significant proportion of distal retro-arc region sources provided sediment based on Paleozoic and Precambrian ages (Finzel et al., 2015). Finzel et al. (2016) suggested that crustal thinning due to thermal erosion from upwelling asthenosphere (Cole and Stewart, 2009; Jacobson et al., 2011; Ling et al., 2013) and temporary arc cessation (Dickinson and Snyder, 1979; Thorkelson, 1996; Gorring and Kay, 2001) associated with passage of the subducting spreading-ridge permitted forearc fluvial systems to expand into the retroarc region.

Modeling results for grains with ages <250 Ma in the middle Eocene strata support arc-derived sediment flux, but point to a

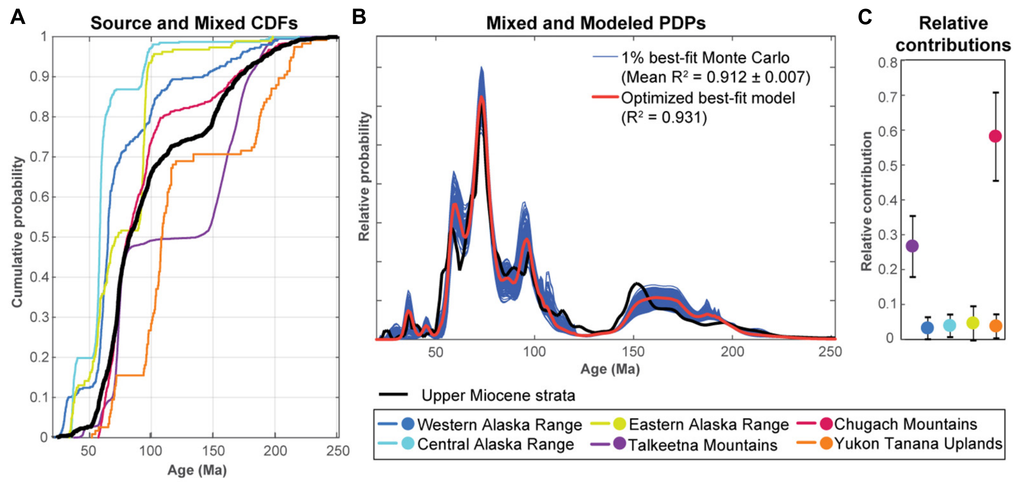

FIGURE 8 | Same as **Figure 3** except for the Upper Miocene strata.

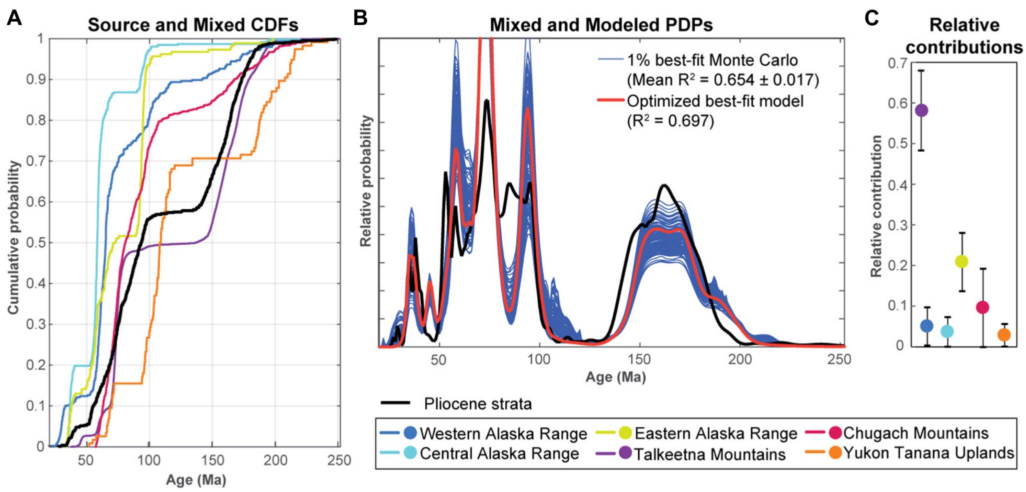

FIGURE 9 | Same as **Figure 3** except for the Pliocene strata.

more specific source from just the western Alaska Range. With an R^2 of 0.902 for the optimized best fit model, it appears as though ∼80% of the <250 Ma zircons can be derived from the western Alaska Range (**Figures 5, 10**). In addition, the PDP of ages from the Eocene strata visually match very closely in age and relative abundance with that from the western Alaska Range, including a significant peak ∼60 Ma, a lesser group of peaks ∼100 Ma, and minor Jurassic populations (**Figure 2**). In comparison, the Eocene strata lack the presence of the large 74 Ma peak present in the Talkeetna Mountains, as well as the ∼94 Ma peak found in the eastern Alaska Range.

Oligocene

Beginning in the late Eocene or early Oligocene (∼35 Ma), the Yakutat microplate began subducting at a shallow angle along the outboard margin of south-central Alaska and continues to the present day (Finzel et al., 2011, 2015; Arkle et al., 2013). Detrital zircon distributions from upper Oligocene (∼27–23 Ma) strata contain Devonian to Mississippian (∼370–340 Ma) and Precambrian (2000–1800 Ma) U-Pb ages, as well as middle Cretaceous (120–90 Ma) zircons with evolved $\varepsilon Hf_{(t)}$ compositions and kyanite in the heavy mineral suite, that indicate continued derivation of sediment from the retroarc Yukon-Tanana Uplands northeast of the present-day Alaska Range.

Modeling results for grains with ages <250 Ma in the upper Oligocene strata again suggest an additional, previously undetected source in the accretionary prism strata of the northern Chugach Mountains, as well as minor contributions from the central Alaska Range (**Figures 6, 10**). Thermochronologic data from the northern Chugach Mountains indicate that exhumation began during late Eocene to early Oligocene time (ca. 35–30 Ma) and continued into early-middle Miocene time (ca. 16–11 Ma; Little and Naeser, 1989; Hoffman and Armstrong, 2006; Arkle et al., 2013; Enkelmann et al., 2019). Exhumation of this region

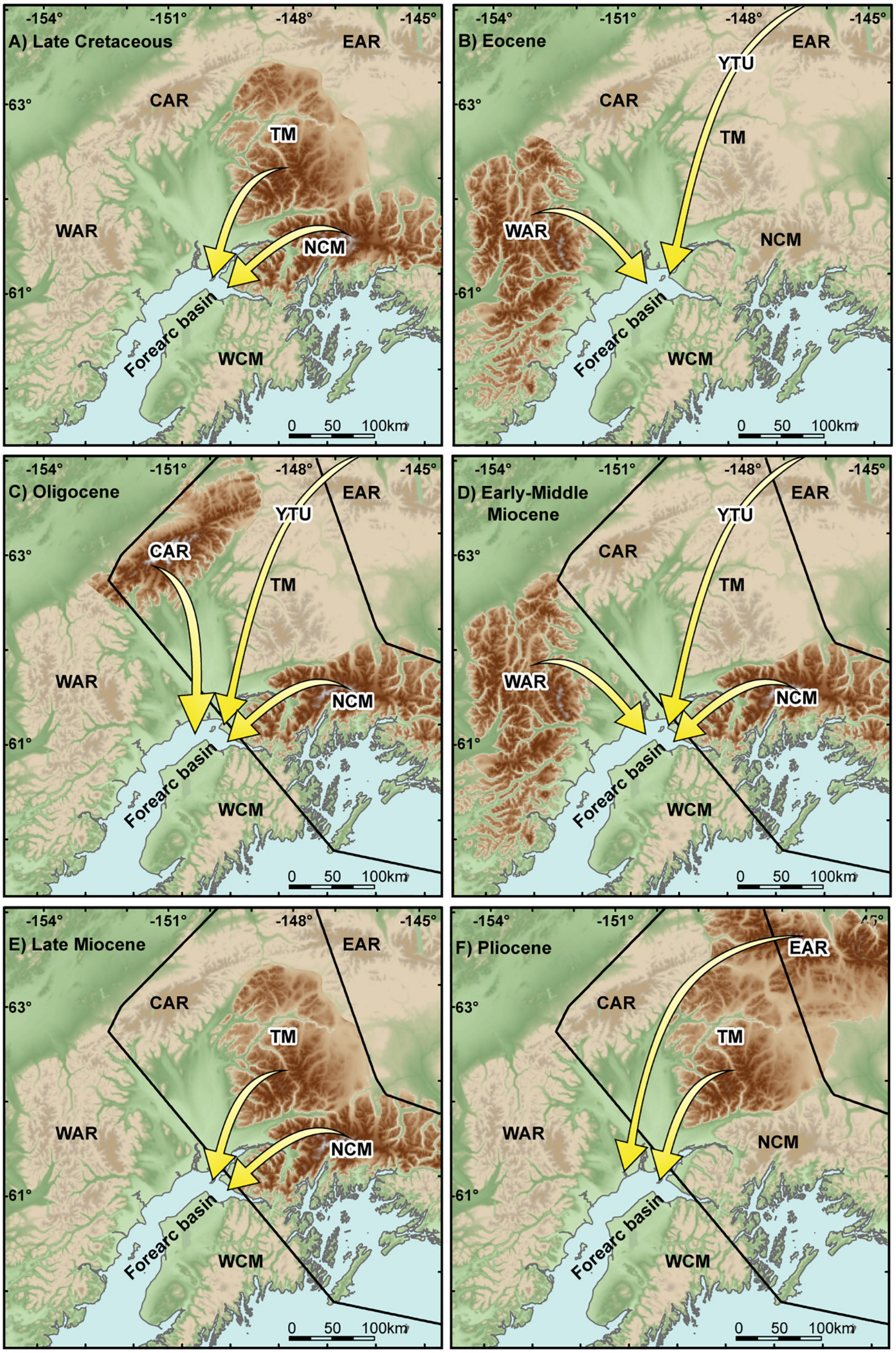

FIGURE 10 | Topographic map of the study area illustrating the predominant sedimentary source regions based on previous interpretations discussed in the text and the modeling results presented here for the **(A)** Late Cretaceous, **(B)** Eocene, **(C)** Oligocene, **(D)** Early-Middle Miocene, **(E)** Late Miocene, and **(F)** Pliocene. The black polygon in **(C–F)** is the present-day position of the Yakutat microplate. Note that forearc strata are contained within the basin, whereas accretionary prism strata are found in the uplifted Chugach Mountain Range. WAR, western Alaska Range; CAR, central Alaska Range; EAR, eastern Alaska Range; TM, Talkeetna Mountains; NCM, northern Chugach Mountains; WCM, western Chugach Mountains; YTU, Yukon Tanana Uplands.

is inferred to reflect initial insertion of the shallow Yakutat slab (Enkelmann et al., 2008, 2010; Finzel et al., 2011, 2015; Arkle et al., 2013). This nascent shallow subduction likely reinvigorated sediment flux from the Chugach accretionary prism into the forearc basin.

Miocene

Shallow subduction of the Yakutat microplate continued during the Miocene. Previous qualitative assessment of detrital zircon U-Pb distributions and $\varepsilon Hf_{(t)}$ values in Lower-Middle Miocene strata suggest that sediment was derived from all margins of the basin, including the central and eastern Alaska Range, western Talkeetna Mountains, and northern Chugach Mountains (Finzel and Enkelmann, 2017). Some of those regions, including the central Alaska Range, western Alaska Range, and eastern Alaska Range produce detrital zircon and apatite fission track ages that reflect late Oligocene to early Miocene (~30–18 Ma) initial and widespread exhumation (Lease et al., 2016; Enkelmann et al., 2019). In addition, apatite thermochronologic ages <20 Ma in the western Chugach Mountains and Talkeetna Mountains indicate exhumation during the Miocene (Little and Naeser, 1989; Hoffman and Armstrong, 2006; Arkle et al., 2013; Valentino et al., 2016). Model results for Lower—Middle Miocene strata have the lowest R^2 of any stratigraphic interval, likely due to undifferentiated weighting of the source signatures, yet the results are consistent with a variety of sediment source regions, including the northern Chugach Mountains and Yukon Tanana Uplands (~30% each) and western and eastern Alaska Ranges (~15% each; **Figures 7, 10**). The widespread nature of the sediment source regions is likely related to coincident shallow subduction beneath south-central Alaska. Crustal thickening due to plateau subduction results in buoyancy and increased coupling between the upper plate and downgoing slab, which drives widespread surface uplift and concentrates stresses in the upper plate that result in strain concentration in rheologically weak zones and triggers significant vertical uplift creating topography and an increase in exhumation rates (Dickinson and Snyder, 1979; Jordan and Allmendinger, 1986; Gutscher et al., 2000; Hampel, 2002; Lallemand et al., 2005; Espurt et al., 2008).

Heavy mineral analyses and sandstone petrography of Upper Miocene strata suggest a provenance area in the Chugach Mountains, with a minor possible contribution from Mesozoic strata located around the flanks of the central Alaska Range (Kirschner and Lyon, 1973; Mongrain, 2012; Helmold et al., 2013; LePain et al., 2013). Detrital zircon U-Pb distributions and $\varepsilon Hf_{(t)}$ values in Upper Miocene strata indicate a dominantly eastern provenance from the northern Chugach and southern Talkeetna Mountains (Finzel and Enkelmann, 2017). The R^2 for the optimized best-fit model of Upper Miocene strata is the highest for any stratigraphic interval and also indicates primary sediment source regions in the northern Chugach Mountains (~60%) and the Talkeetna Mountains (~30%; **Figures 8, 10**). Both of these areas lie above the modern-day flat-slab region (**Figure 1**). The Yakutat microplate is interpreted as a wedge-shaped oceanic plateau that thickens from ~11 km at its deepest observable extent in the mantle to ~30 km thick at the modern coastline (Ferris et al., 2003; Eberhart-Phillips et al., 2006; Worthington et al., 2008, 2012; Christeson et al., 2010; Bauer et al., 2014). Therefore, as subduction of the microplate has progressed, increasingly thicker crust has been inserted beneath south-central Alaska, resulting in an overall inboard migration of exhumation and sediment bypass above the flat-slab region, and a relative increase in sediment flux toward areas adjacent to the flat-slab region (Finzel et al., 2011).

Pliocene

Previous assessment of detrital zircon U-Pb distributions and $\varepsilon Hf_{(t)}$ values in Pliocene strata indicate a continuation of a dominantly eastern provenance including the northern Chugach and southern Talkeetna Mountains, as well as a smaller sediment flux from the Alaska Range (Finzel and Enkelmann, 2017). Model results for Pliocene strata have the second lowest R^2 of any stratigraphic interval, probably again due to undifferentiated weighting of the source signatures, but still agree with previous interpretations. The relative contributions for the Pliocene strata are modeled as ~60% from the Talkeetna Mountains, ~20% from the eastern Alaska Range, and ~10% from the northern Chugach Mountains (**Figures 9, 10**). This overall inboard shift in sediment source regions is consistent with progressively thicker portions of the Yakutat microplate being inserted beneath south-central Alaska and triggering exhumation in farther inboard source regions as a result.

DISCUSSION

Forearc Basin Response to External Tectonic Forcing

The southern margin of Alaska has experienced convergence and subduction since at least Jurassic time, resulting in prolonged magmatism that produced geographically extensive plutonic belts with different ages that often spatially overlap, making provenance determination as it relates to the complex tectonic history of the region difficult. The combined analysis of detrital zircon sampling of modern rivers and basin strata in conjunction with mixture modeling, however, presents a useful method for partitioning the widespread and pervasive zircon ages in the sediment source regions, permitting a more nuanced resolution of the tectonic forcing on the sedimentary systems. For example, evaluation of the model results reveals a predominance of sediment input from the Talkeetna Mountains during the Early Cretaceous (**Figure 11**). This time marks a period of ongoing accretion between the Insular terranes and the western margin of North America (Pavlis, 1982; McClelland et al., 1992; Trop et al., 2002, 2005; Manuszak et al., 2007). Early Cretaceous exhumation of the northern Talkeetna Mountains in response to accretion is recorded in spatially restricted non-marine Aptian—Cenomanian strata that unconformably overlie marine Jurassic-Cretaceous strata (Hampton et al., 2007). Therefore, contraction and exhumation of the Talkeetna Mountains due to collision of the Insular terranes resulted in that region being a primary sediment source for the forearc basin during Early Cretaceous time.

Terminal suturing of the terranes occurred during the Late Cretaceous (~84–67 Ma) in south-central Alaska

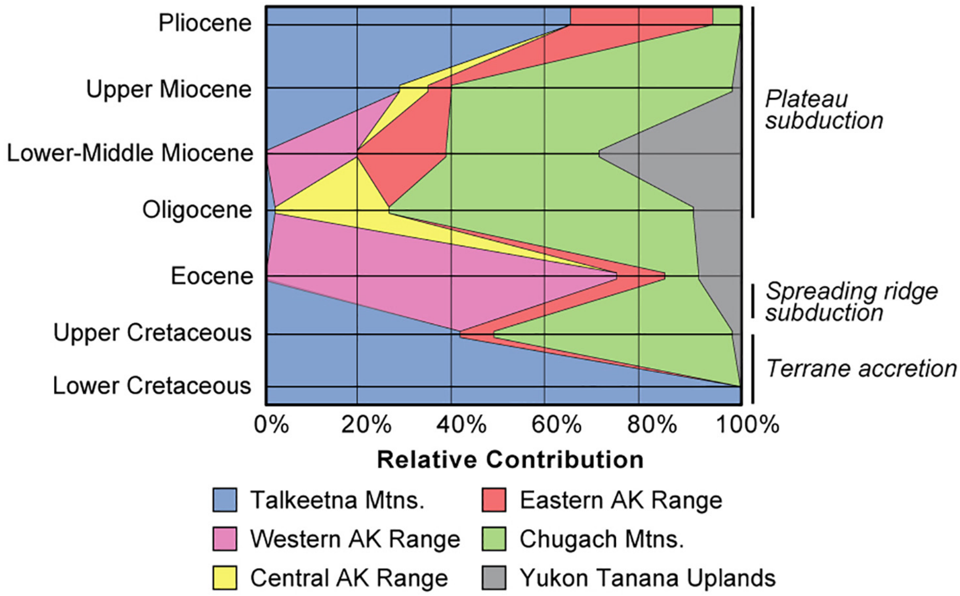

FIGURE 11 | Graph depicting temporal variations in relative contributions from the potential source regions in southern Alaska.

(Trop et al., 2019). Upper Cretaceous strata record the addition of a new source region in the Chugach Mountains, and to a much lesser extent, the eastern Alaska Range and Yukon-Tanana Uplands (**Figure 11**). A prominent 98 Ma zircon fission track peak from modern rivers draining the Talkeetna Mountains reveals ongoing exhumation in that region (Enkelmann et al., 2019). Late Cretaceous exhumation of the accretionary prism could be related to changes in plate kinematics induced by final suturing of the Insular terranes. Relative convergent plate motions between the terranes and the subducting plate that were previously partly accommodated by migration of the terranes toward North America must have been transferred elsewhere as the terranes were juxtaposed against the continental backstop. That convergence may have focused contractional deformation to the outboard margin of the terranes and contributed to the overall uplift of the accretionary prism strata.

By Eocene time, after the passage of a subducting spreading ridge or break-off of the subducting slab, the dominant sediment source region was the western Alaska Range with lesser contributions from the eastern Alaska Range, Chugach Mountains, and Yukon Tanana Uplands (**Figure 11**). Zircon and apatite fission track data from modern rivers sourced in the western Alaska Range record exhumation of that region during the Paleocene and Eocene, but the driving factors remain debated. By the Oligocene, however, the dominant sediment source area was again the Chugach Mountains with smaller contributions from the central Alaska Range and Yukon Tanana Uplands. Initiation of shallow subduction of the Yakutat microplate is inferred to have triggered uplift and exhumation in the Chugach Mountains (Arkle et al., 2013; Ferguson et al., 2015) and across the entire Alaska Range, which is also recorded in synorogenic Oligocene strata in the central Alaska Range (Benowitz et al., 2011, 2012, 2014; Fitzgerald et al., 2014; Riccio et al., 2014; Lease et al., 2016; Enkelmann et al., 2019; Terhune et al., 2019; Trop et al., 2019).

Shallow subduction strongly influenced sediment flux into the forearc basin, either turning off or completely swamping any sediment input from the formerly important inboard source regions in the Talkeetna Mountains and western Alaska Range with new renewed contributions from the Chugach Mountains. In fact, major contributions from the Chugach Mountains appear to be intricately linked to plate margin events. For example, during the final suturing of the Insular terranes in the Late Cretaceous, the Chugach Mountains were triggered as a primary sediment source region. Then again during insertion of the shallow slab in the Oligocene, sediment flux from that range was rejuvenated. As the shallow slab was progressively inserted beneath south-central Alaska during the Miocene-Pliocene, it continued to force changes in sediment source regions. Outboard sediment sources from the Chugach Mountains were progressively overwhelmed by more inboard sediment sources including the Talkeetna Mountains and eastern Alaska Range. It is clear that tectonic forcing on the forearc region has played a significant role in source region exhumation and sediment routing since Cretaceous time.

Benefits and Limitations of the Watershed Approach

Using sediment from modern drainage systems to constrain ancient sediment source regions has many advantages. Detrital zircon grains in modern rivers are derived from all available bedrock sources in a watershed. Dating of those grains provides a quick and efficient way to characterize the distribution of ages present in potential source areas. This is especially important in regions that are underexplored or difficult to access. Modern river sampling also provides a unique opportunity to assess sediment recycling in a basin. A major difficulty associated with detrital zircons is that they are very robust and can remain intact for several sedimentary cycles. Consequently, recycling of detrital zircons from older strata is often a concern but cannot be adequately addressed due to poor characterization of older stratigraphic successions. Characterizing the detrital signature of multiple older successions would be costly and time-consuming, especially considering that the detrital zircon signature within an individual stratigraphic unit can vary greatly. In contrast, careful selection of watersheds and sampling sites allows rapid characterization of exhumed stratigraphic units. Combined with mixture modeling, this is a powerful tool to assess recycled versus primary sediment input into a basin.

The watershed approach also has limitations. For example, exposure of various bedrock units or the geometries of catchments may have varied over time. Therefore, it is important to constrain the landscape evolution of the potential source regions adjacent to a sedimentary basin in order to produce robust results. In south-central Alaska, significant changes to most of the landscape have not occurred during much of Cenozoic time. Combined U-Pb and fission track double-dating of detrital zircon from modern rivers in the Talkeetna and Chugach Mountains reveals a preponderance of unreset, magmatic zircon grains with Jurassic and Late Cretaceous ages, suggesting limited amounts of exhumation of those regions during Cenozoic time (Enkelmann et al., 2019). Furthermore, Terhune et al. (2019) suggest that significant paleotopography in the Talkeetna Mountains was created by Paleocene time based on $^{40}Ar/^{39}Ar$, apatite fission track, and apatite (U-Th)/He cooling ages, but the region has not experienced much exhumation since then. Minor and localized Miocene cooling ages there are geographically restricted to proximity with the active Castle Mountain fault. Probably the only regions that have experienced a noteworthy change in topography is the central and eastern Alaska Ranges, which have been uplifting since ∼30–25 Ma (Benowitz et al., 2011, 2012, 2014; Fitzgerald et al., 2014; Riccio et al., 2014; Lease et al., 2016).

CONCLUSION

The unified approach of extensive modern river sampling to characterize sediment source regions, comprehensive basin strata characterization, and mixture modeling demonstrates a valuable approach for not only apportioning of widespread and pervasive ages found in source terranes with long-lived magmatic histories, but also for resolving sedimentary recycling into a basin. In south-central Alaska, mixture modeling of the extensive detrital zircon U-Pb geochronologic dataset presented here provides an opportunity to more fully characterize the long-term variations of provenance within a forearc basin. Modeling of only the <250 Ma age component of the detrital zircon signatures reveals a previously undetected sediment source in recycling of the accretionary prism strata in the northern Chugach Mountains during the Late Cretaceous and Oligocene. Recognition of this important sediment source was previously hampered by overlap of detrital zircon U-Pb ages in the ancient strata with widespread igneous belts north of the basin. Rejuvenation of sediment flux from the Chugach Mountains can be linked to specific plate margin events, including Late Cretaceous suturing of the Insular terranes and Oligocene initiation of shallow subduction. The results of this analysis permit a better understanding of the tectonic forcing that influences sediment derivation and dispersal along active tectonic margins. This study also demonstrates that in basins where the topographic and exhumational evolution of provenance regions is well-constrained, strategically using sediment from modern rivers is a formidable technique to rapidly and efficiently characterize vast sediment source regions for resolving provenance of ancient strata.

DATA AVAILABILITY

The datasets generated for this study can be found in the **Supplementary Material**.

AUTHOR CONTRIBUTIONS

EF analyzed the data and wrote the manuscript.

FUNDING

This research was funded through NSF-EAR 1419683. Support for the University of Arizona LaserChron Center, where the geochronologic data was collected, is provided through NSF-EAR 1649254.

ACKNOWLEDGMENTS

The new data from the Talkeetna Mountains was collected in collaboration with Eva Enkelmann (University of Calgary) for an MS thesis written by Carsyn Ames at the University of Iowa. Enkelmann also provided valuable feedback on the manuscript.

SUPPLEMENTARY MATERIAL

The Supplementary Material for this article can be found online at: https://www.frontiersin.org/articles/10.3389/feart.2019.00217/full#supplementary-material

DATA SHEET S1 | The supplementary file associated with this manuscript contains reference and sample number information about the compiled data, age distributions used for each source area and stratigraphic interval used in the modeling, and raw isotopic data for the 20 new river samples from the Talkeetna Mountains.

REFERENCES

Arkle, J., Armstrong, P., Haeussler, P., Prior, M., Hartman, S., Sendziak, K., et al. (2013). Focused exhumation in the syntaxis of the western Chugach Mountains and Prince William Sound, Alaska. *Geol. Soc. Am. Bull.* 125, 776–793. doi: 10.1130/b30738.1

Bacon, C., Vazquez, J., and Wooden, J. (2012). Peninsular terrane basement ages recorded by paleozoic and paleoproterozoic zircon in gabbro xenoliths and andesite from Redoubt volcano, Alaska. *Geol. Soc. Am. Bull.* 124, 24–34. doi: 10.1130/b30439.1

Bauer, M., Pavlis, G., and Landes, M. (2014). Subduction geometry of the yakutat terrane, southeastern Alaska. *Geosphere* 10, 1161–1176. doi: 10.1130/ges00852.1

Benowitz, J. A., Haeussler, P. J., Layer, P. W., O'Sullivan, P. B., Wallace, W. K., and Gillis, R. J. (2012). Cenozoic tectono-thermal history of the Tordrillo Mountains, Alaska: paleocene-eocene ridge subduction, decreasing relief, and late Neogene faulting. *Geochem. Geophys. Geosyst.* 13:Q04009. doi: 10.1029/2011GC003951

Benowitz, J. A., Layer, P. W., Armstrong, P., Perry, S., Haeussler, P. J., Fitzgerald, P., et al. (2011). Spatial variations in focused exhumation along a continental-scale strike-slip fault: the Denali fault of the Eastern Alaska Range. *Geosphere* 7, 455–467. doi: 10.1130/GES00589.1

Benowitz, J. A., Layer, P. W., and Vanlaningham, S. (2014). "Persistent long-term (c. 24 Ma) exhumation in the Eastern Alaska Range constrained by stacked thermochronology," in *Advances in 40Ar/39Ar Dating: From Archeology to Planetary Sciences*, Vol. 378, eds F. Jourdan, D. F. Mark, and C. Verati, (London: Geological Society of London), 225–243. doi: 10.1144/sp378.12

Blodgett, R., and Sralla, B. (2008). "A major unconformity between Permian and Triassic strata at Cape Kekurnoi, Alaska Peninsula; old and new observations on stratigraphy and hydrocarbon potential," in *Studies by the U.S. Geological Survey in Alaska, 2006: U.S. Geological Survey Professional Paper 1739-E*, eds P. Haeussler, and J. Galloway, (Reston, VA: U.S. Geological Survey), 13.

Bradley, D., Kusky, T., Haeussler, P., Goldfarb, R., Miller, M., Dumoulin, J., et al. (2003). "Geologic signature of early tertiary ridge subduction in Alaska," in *Geology of a transpressional orogen developed during ridge-trench interaction along the north Pacific margin*, eds V. Sisson, S. Roekse, and T. Pavlis, (Boulder, CO: Geological Society of America), 19–49. doi: 10.1130/0-8137-2371-x.19

Butler, R., Gehrels, G., and Bazard, D. (1997). Paleomagnetism of paleozoic strata of the alexander terrane, southeastern Alaska. *Geol. Soc. Am. Bull.* 109, 1372–1388. doi: 10.1130/0016-76061997109<1372:Popsot<2.3.Co;2

Calderwood, K., and Fackler, W. (1972). Proposed stratigraphic nomenclature for Kenai Group, Cook Inlet basin, Alaska. *Am. Assoc. Petrol. Geol. Bull.* 56, 739–754.

Christeson, G., Gulick, S., van Avendonk, H., Worthington, L., Reece, R., and Pavlis, T. (2010). The yakutat terrane: dramatic change in crustal thickness across the Transition fault, Alaska. *Geology* 38, 895–898. doi: 10.1130/g31170.1

Clift, P., Draut, A., Kelemen, P., Blusztajn, J., and Greene, A. (2005). Stratigraphic and geochemical evolution of an oceanic arc upper crustal section: the jurassic talkeetna volcanic formation, south-central Alaska. *Geol. Soc. Am. Bull.* 117, 1368–1373.

Cole, R., Nelson, S., Layer, P., and Oswald, P. (2006). Eocene volcanism above a depleted mantle slab window in southern Alaska. *Geol. Soc. Am. Bull.* 118, 140–158. doi: 10.1130/b25658.1

Cole, R., and Stewart, B. (2009). Continental margin volcanism at sites of spreading ridge subduction: examples from southern Alaska and western California. *Tectonophysics* 464, 118–136. doi: 10.1016/j.tecto.2007.12.005

Cowan, D., Brandon, M., and Garver, J. (1997). Geologic tests of hypotheses for large coastwise displacements - A critique illustrated by the Baja British Columbia controversy. *Am. J. Sci.* 297, 117–173. doi: 10.2475/ajs.297.2.117

Davidson, C., and McPhillips, D. (2007). "Along strike variations in metamorphism and deformation of the strata of the Kahiltna basin, south-central Alaska," in *Tectonic Growth of a Collisional Continental Margin: Crustal Evolution of Southern Alaska*, eds K. Ridgway, J. Trop, J. Glen, and J. O'Neill, (Boulder, CO: Geological Society of America), 439–453. doi: 10.1130/2007.2431(17)

DeCelles, P., Gehrels, G., Quade, J., Ojha, T., Kapp, P., and Upreti, B. (1998). Neogene foreland basin deposits, erosional unroofing, and the kinematic history of the Himalayan fold-thrust belt, western Nepal. *Geol. Soc. Am. Bull.* 110, 2–21. doi: 10.1130/0016-76061998110<0002:Nfbdeu<2.3.Co;2

DeGraaff-Surpless, K., Graham, S., Wooden, J., and McWilliams, M. (2002). Detrital zircon provenance analysis of the Great Valley Group, California: evolution of an arc-forearc system. *Geol. Soc. Am. Bull.* 114, 1564–1580. doi: 10.1130/0016-76062002114<1564:Dzpaot<2.0.Co;2

Dickinson, W., and Gehrels, G. (2009). Use of U-Pb ages of detrital zircons to infer maximum depositional ages of strata: a test against a Colorado Plateau Mesozoic database. *Earth Planet. Sci. Lett.* 288, 115–125. doi: 10.1016/j.epsl.2009.09.013

Dickinson, W., and Snyder, W. (1979). Geometry of subducted slabs related to San-Andreas transform. *J. Geol.* 87, 609–627. doi: 10.1086/628456

Eastham, K., and Ridgway, K. (2002). "Stratigraphy and provenance data from the Upper Jurassic to Upper Cretaceous Kahiltna assemblage of south-central Alaska," in *Studies by the U.S. Geological Survey in Alaska, 2000: U.S. Geological Survey Professional Paper 1662*, eds F. Wilson, and J. Galloway, (Reston, VA: U.S. Geological Suvery), 45–53.

Eberhart-Phillips, D., Christensen, D., Brocher, T., Hansen, R., Ruppert, N., Haeussler, P., et al. (2006). Imaging the transition from Aleutian subduction to Yakutat collision in central Alaska, with local earthquakes and active source data. *J. Geophys. Res. Solid Earth* 111:B11303. doi: 10.1029/2005jb004240

Enkelmann, E., Garver, J., and Pavlis, T. (2008). Rapid exhumation of ice-covered rocks of the Chugach-St. *Elias orogen*, Southeast Alaska. *Geology* 36, 915–918. doi: 10.1130/g2252a.1

Enkelmann, E., Lohff, S. K. S., and Finzel, E. S. (2019). Detrital zircon double-dating of forearc basin strata reveals magmatic, exhumational, and thermal history of sediment source areas. *Geol. Soc. Am. Bull.* 131, 1364–1384. doi: 10.1130/B35043.1

Enkelmann, E., Zeitler, P., Garver, J., Pavlis, T., and Hooks, B. (2010). The thermochronological record of tectonic and surface process interaction at the Yakutat-North American collision zone in southeast Alaska. *Am. J. Sci.* 310, 231–260. doi: 10.2475/04.2010.01

Espurt, N., Funiciello, F., Martinod, J., Guillaume, B., Regard, V., Faccenna, C., et al. (2008). Flat subduction dynamics and deformation of the South American plate: insights from analog modeling. *Tectonics* 27:TC3011. doi: 10.1029/2007TC002175

Fedo, C., Sircombe, K., Rainbird, R., Hanchar, J., and Hoskin, P. (2003). Detrital zircon analysis of the sedimentary record. *Rev. Mineral. Geochem.* 53, 277–303. doi: 10.2113/0530277

Ferguson, K. M., Armstrong, P. A., Arkle, J. C., and Haeussler, P. J. (2015). Focused rock uplift above the subduction decollement at Montague and Hinchinbrook Islands, Prince William Sound, Alaska. *Geosphere* 11, 144–159. doi: 10.1130/GES01036.1

Ferris, A., Abers, G., Christensen, D., and Veenstra, E. (2003). High resolution image of the subducted Pacific (?) plate beneath central Alaska, 50-150 km depth. *Earth Planet. Sci. Lett.* 214, 575–588. doi: 10.1016/s0012-821x(03)00403-5

Finzel, E., and Enkelmann, E. (2017). Miocene-Recent sediment flux in the south-central Alaskan fore-arc basin governed by flat-slab subduction. *Geochem. Geophys. Geosyst.* 18, 1739–1760. doi: 10.1002/2016gc006783

Finzel, E., Enkelmann, E., Falkowski, S., and Hedeen, T. (2016). Long-term fore-arc basin evolution in response to changing subduction styles in southern Alaska. *Tectonics* 35, 1735–1759. doi: 10.1002/2016tc004171

Finzel, E., Ridgway, K., and Trop, J. (2015). Provenance signature of changing plate boundary conditions along a convergent margin: detrital record of spreading-ridge and flat-slab subduction processes, Cenozoic forearc basins, Alaska. *Geosphere* 11, 823–849. doi: 10.1130/ges01029.1

Finzel, E., Trop, J., Ridgway, K., and Enkelmann, E. (2011). Upper plate proxies for flat-slab subduction processes in southern Alaska. *Earth Planet. Sci. Lett.* 303, 348–360. doi: 10.1016/j.epsl.2011.01.014

Fitzgerald, P. G., Roeske, S. M., Benowitz, J. A., Riccio, S. J., Perry, S. E., and Armstrong, P. A. (2014). Alternating asymmetric topography of the Alaska range along the strike-slip Denali fault: strain partitioning and lithospheric control across a terrane suture zone. *Tectonics* 33, 1519–1533. doi: 10.1002/2013TC003432

Flores, R., Stricker, G., and Kinney, S. (2004). Alaska coal geology, resources, and coalbed methane potential. *U.S. Geol. Surv. Digit. Data Ser.* 77:68.

Gehrels, G. (2012). "Detrital zircon U-Pb geochronology: current methods and new opportunities," in *Tectonics of Sedimentary Basins: Recent Advances*, eds C. Busby, and A. Azor, (Hoboke, NJ: Blackwell Science Publication).

Gehrels, G., Valencia, V., and Pullen, A. (2006). Detrital zircon geochronology by laser ablation multicollector ICPMS at the arizona laserchron center. *Paleontol. Soc. Pap.* 12, 67–76. doi: 10.1017/s1089332600001352

Gehrels, G., Valencia, V., and Ruiz, J. (2008). Enhanced precision, accuracy, efficiency, and spatial resolution of U-Pb ages by laser ablation-multicollector-inductively coupled plasma-mass spectrometry. *Geochem. Geophys. Geosyst.* 9:Q03017. doi: 10.1029/2007gc001805

Gorring, M., and Kay, S. (2001). Mantle processes and sources of neogene slab window magmas from southern Patagonia, Argentina. *J. Petrol.* 42, 1067–1094. doi: 10.1093/petrology/42.6.1067

Grantz, A. (1960). *Geologic Map and Cross Section of Talkeetna Mountains (A-1) Quadrangle and the South Third of Talkeetna Mountains (B-1) Quadrangle, Alaska*. Reston, VA: U.S. Geological Survey.

Gutscher, M. A., Spakman, W., Bijwaard, H., and Engdahl, E. R. (2000). Geodynamics of flat subduction: seismicity and tomographic constraints from the Andean margin. *Tectonics* 19, 814–833. doi: 10.1029/1999TC001152

Haeussler, P., Bradley, D., Wells, R., and Miller, M. (2003). Life and death of the Resurrection plate: evidence for its existence and subduction in the northeastern Pacific in Paleocene-Eocene time. *Geol. Soc. Am. Bull.* 115, 867–880. doi: 10.1130/0016-76062003115<0867:Ladotr<2.0.Co;2

Hampel, A. (2002). The migration history of the Nazca Ridge along the Peruvian active margin: a re-evaluation. *Earth Planet. Sci. Lett.* 203, 665–679. doi: 10.1016/S0012-821X(02)00859-2

Hampton, B., Ridgway, K., O'Neill, J., Gehrels, G., Schmidt, J., and Blodgett, R. (2007). " Pre-, syn-, and postcollisional stratigraphic framework and provenance of upper triassic-upper cretaceous strata in the northwestern Talkeetna Mountains, Alaska," in *Tectonic Growth of a Collisional Continental Margin: Crustal Evolution of Southern Alaska*, eds K. Ridgway, J. Trop, J. Glen, and J. O'Neill, (Boulder, CO: Geological Society of America), 401–438. doi: 10.1130/2007.2431(16)

Helmold, K., LePain, D., Wilson, M., and Peterson, C. (2013). *Petrology and reservoir potential of Tertiary and Mesozoic sandstones, Cook Inlet, Alaska: A preliminary analysis of outcrop samples collected during 2007-2010 field seasons*. Alaska Division of Geological & Geophysical Surveys Preliminary Interpretive Report 2013-5. Fairbanks, AK: Alaska Division of Geological & Geophysical Surveys, 34.

Hoffman, M., and Armstrong, P. (2006). "Miocene exhumation of the southern Talkeetna Mountains, south central Alaska, based on apatite (U-Th)/He thermochronology," in *Proceeding of the GSA Abstracts with Programs*, (Boulder, CO: Geological Society of America).

Houston, W. (1994). *Lower Tertiary stratigraphy in Katmai National Park, Alaska-a lithologic and petrographic study*. M.S. Thesis, Colorado State University, Fort Collins, CO.

Irving, E., Woodsworth, G., Wynne, P., and Morrison, A. (1985). Paleomagnetic evidence for displacement from the south of the coast plutonic complex, British-Columbia. *Can. J. Earth Sci.* 22, 584–598. doi: 10.1139/e85-058

Irving, E., Wynne, P., Thorkelson, D., and Schiarizza, P. (1996). Large (1000 to 4000 km) northward movements of tectonic domains in the northern Cordillera, 83 to 45 Ma. *J. Geophys. Res. Solid Earth* 101, 17901–17916. doi: 10.1029/96jb01181

Jacobson, C., Grove, M., Pedrick, J., Barth, A., Marsaglia, K., Gehrels, G., et al. (2011). Late Cretaceous-early Cenozoic tectonic evolution of the southern California margin inferred from provenance of trench and forearc sediments. *Geol. Soc. Am. Bull.* 123, 485–506. doi: 10.1130/b30238.1

Jones, D., and Silberling, N. (1979). *Mesozoic stratigraphy; the key to tectonic analysis of southern and central Alaska*. U.S. Geological Survey Open-File Report79-1200.

Jones, D., Silberling, N., and Hillhouse, J. (1977). Wrangellia - displaced terrane in northwestern North-America. *Can. J. Earth Sci.* 14, 2565–2577. doi: 10.1139/e77-222

Jordan, T. E., and Allmendinger, R. W. (1986). The Sierras pampeanas of argentina - a modern analog of rocky-mountain foreland deformation. *Am. J. Sci.* 286, 737–764. doi: 10.2475/ajs.286.10.737

Kalbas, J., Ridgway, K., and Gehrels, G. (2007). "Stratigraphy, depositional systems, and provenance of the lower cretaceous kahiltna assemblage, western Alaska Range: basin development in response to oblique collision," in *Tectonic Growth of a Collisional Continental Margin: Crustal Evolution of Southern Alaska*, eds K. Ridgway, J. Trop, J. Glen, and J. O'Neill, (Boulder, CO: Geological Society of America), 307–343. doi: 10.1130/2007.2431(13)

Keppie, J., and Dostal, J. (2001). Evaluation of the Baja controversy using paleomagnetic and faunal data, plume magmatism, and piercing points. *Tectonophysics* 339, 427–442. doi: 10.1016/s0040-1951(01)00126-3

Kirschner, C., and Lyon, C. (1973). Stratigraphic and tectonic development of Cook Inlet petroleum province. *Am. Assoc. Petrol. Geol. Bull.* 19, 396–407.

Lallemand, S., Heuret, A., and Boutelier, D. (2005). On the relationships between slab dip, back-arc stress, upper plate absolute motion, and crustal nature in subduction zones. *Geochem. Geophys. Geosyst.* 6:Q09006. doi: 10.1029/2005GC000917

Lease, R., Haeussler, P., and O'Sullivan, P. (2016). Changing exhumation patterns during Cenozoic growth and glaciation of the Alaska Range: insights from detrital thermochronology and geochronology. *Tectonics* 35, 934–955. doi: 10.1002/2015tc004067

LePain, D., Stanley, R., Helmold, K., and Shellenbaum, D. (2013). "Geologic framework and petroleum systems of Cook Inlet Basin, south-central Alaska," in *Oil and Gas Fields fo the Cook Inlet Basin, Alaska*, eds D. Stone, and D. Hite, (Tulsa, OK: American Association of Petroleum Geologists), 37–116.

Ling, M., Li, Y., Ding, X., Teng, F., Yang, X., Fan, W., et al. (2013). Destruction of the North China craton induced by ridge subductions. *J. Geol.* 121, 197–213. doi: 10.1086/669248

Little, T., and Naeser, C. (1989). Tertiary tectonics of the border ranges fault system, Chugach Mountains, Alaska - deformation and uplift in a fore-arc setting. *J. Geophys. Res. Solid Earth Planets* 94, 4333–4359. doi: 10.1029/JB094iB04p04333

Magoon, L., Adkison, W., Chmelik, F., Dolton, G., Fisher, M., Hampton, M., et al. (1976). *Hydrocarbon Potential, Geologic Hazards, and Infrastructure for Exploration and Development of the Lower Cook Inlet, Alaska*. Open-File Report 97-26. Reston, VA: U.S. Geological Survey.

Magoon, L., and Egbert, R. (1986). "Framework geology and sandstone composition," in *Geologic studies of the lower Cook Inlet COST No. 1 well, Alaska Outer Continental Shelf*, ed. L. Magoon, (Reston, VA: U.S. Geological Survey), 17–22.

Manuszak, J., Ridgway, K., Trop, J., and Gehrels, G. (2007). "Sedimentary record of the tectonic growth of a collisional continental margin: upper jurassic-lower cretaceous nutzotin mountains sequence, eastern Alaska Range, Alaska," in *Tectonic Growth of a Collisional Continental Margin: Crustal Evolution of Southern Alaska*, eds K. Ridgway, J. Trop, J. Glen, and J. O'Neill, (Boulder, CO: Geological Society of America), 345–377. doi: 10.1130/2007.2431(14)

McClelland, W., Gehrels, G., and Saleeby, J. (1992). Upper jurassic-lower cretaceous basinal strata along the cordilleran margin - implications for the accretionary history of the alexander-wrangellia-peninsular terrane. *Tectonics* 11, 823–835. doi: 10.1029/92tc00241

Mongrain, J. (2012). *Depositional systems, paleoclimate, and provenance of the Late Miocene to Pliocene Beluga and Sterling Formations, Cook Inlet forearc basin, Alaska*. Ph.D. Thesis, University of Alaska, Anchorage, AK.

Nokleberg, W., Aleinikoff, J., Dutro, J., Lanphere, M., Silberling, N., Silva, S., et al. (1992). *Map, Tables, and Summary of Fossil and Isotopic Age Data, Mount Hayes Quadrangle, Eastern Alaska Range*. Reston, VA: U.S. Geological Survey.

Nokleberg, W., Parfenov, L., Monger, J., Norton, I., Khanchuk, A., Stone, D., et al. (2001). Phanerozoic tectonic evolution of the Circum-North Pacific. *U.S. Geol. Surv. Prof. Pap.* 1626:122.

Panuska, B. (1985). Paleomagnetic evidence for a post-Cretaceous accretion of Wrangellia. *Geology* 13, 880–883. doi: 10.1130/0091-7613198513<880:Pefapa<2.0.Co;2

Pavlis, T. (1982). Origin and age of the Border Ranges Fault of southern Alaska and its bearing on the late Mesozoic tectonic evolution of Alaska. *Tectonics* 1, 343–368. doi: 10.1029/TC001i004p00343

Plafker, G., Moore, J., and Winkler, G. (1994). "Geology of the southern Alaska margin," in *Geology of North America*, eds G. Plafker, and H. Berg, (Boulder, CO: Geological Society of America), 389–448.

Plafker, G., Nokleberg, W., and Lull, J. (1989). Bedrock geology and tectonic evolution of the wrangellia, peninsular, and chugach terranes along the trans-alaska crustal transect in the Chugach Mountains and southern Copper River Basin, Alaska. *J. Geophys. Res. Solid Earth Planets* 94, 4255–4295. doi: 10.1029/JB094iB04p04255

Pullen, A., Ibanez-Mejia, M., Gehrels, G., Ibanez-Mejia, J., and Pecha, M. (2014). What happens when n= 1000? Creating large-n geochronological datasets with

LA-ICP-MS for geologic investigations. *J. Analyt. Atom. Spectrom.* 29, 971–980. doi: 10.1039/c4ja00024b

Reid, M., Finzel, E., Enkelmann, E., and McClelland, W. (2018). "Detrital zircon provenance of upper jurassic–upper cretaceous forearc basin strata on the insular terranes, south-central Alaska," in *Tectonics, Sedimentary Basins, and Provenance: A Celebration of William R. Dickinson's Career*, eds R. Ingersoll, T. Lawton, and S. Graham, (Boulder, CO: Geological Society of America), 571–590.

Riccio, S. J., Fitzgerald, P. G., Benowitz, J. A., and Roeske, S. M. (2014). The role of thrust faulting inthe formation of the eastern Alaska Range: Thermochronological constraints from the Susitna Glacier Thrust Fault region of the intracontinental strike-slip Denali Fault sys-tem. *Tectonics* 33, 2195–2217. doi: 10.1002/2014TC003646

Ridgway, K., Trop, J., Nokleberg, W., Davidson, C., and Eastham, K. (2002). Mesozoic and Cenozoic tectonics of the eastern and central Alaska Range: progressive basin development and deformation in a suture zone. *Geol. Soc. Am. Bull.* 114, 1480–1504. doi: 10.1130/0016-76062002114<1480:Mactot<2.0.Co;2

Ridgway, K., Trop, J., and Sweet, A. (1997). Thrust-top basin formation along a suture zone, Cantwell basin, Alaska range: implications for development of the Denali fault system. *Geol. Soc. Am. Bull.* 109, 505–523. doi: 10.1130/0016-76061997109<0505:Ttbfaa<2.3.Co;2

Rioux, M., Hacker, B., Mattinson, J., Kelemen, P., Blusztajn, J., and Gehrels, G. (2007). Magmatic development of an intra-oceanic arc: high-precision U-Pb zircon and whole-rock isotopic analyses from the accreted Talkeetna arc, south-central Alaska. *Geol. Soc. Am. Bull.* 119, 1168–1184. doi: 10.1130/b25964.1

Rioux, M., Mattinson, J., Hacker, B., Kelemen, P., Blusztajn, J., Hanghoj, K., et al. (2010). Intermediate to felsic middle crust in the accreted Talkeetna arc, the Alaska Peninsula and Kodiak Island, Alaska: an analogue for low-velocity middle crust in modern arcs. *Tectonics* 29:TC3001. doi: 10.1029/2009tc002541

Sisson, V., Poole, A., Burner, H., Pavlis, T., Copeland, P., Donelick, R., et al. (2003). "Geochemical and geochronologic constraints for genesis of a tonalite-trondhjemite suite and associated mafic intrusive rocks in the eastern Chugach Mountains, Alaska: a record of ridge-transform subduction," in *Geology of a Transpressional Orogen Developed During Ridge-Trench Interaction Along the North Pacific Margin*, eds V. Sisson, S. Roekse, and T. Pavlis, (Boulder, CO: Geological Society of America), 293–326. doi: 10.1130/0-8137-2371-x.293

Stamatakos, J., Trop, J., and Ridgway, K. (2001). Late Cretaceous paleogeography of Wrangellia: paleomagnetism of the MacColl Ridge Formation, southern Alaska, revisited. *Geology* 29, 947–950. doi: 10.1130/0091-76132001029<0947:Lcpowp<2.0.Co;2

Sundell, K., and Saylor, J. (2017). Unmixing detrital geochronology age distributions. *Geochem. Geophys. Geosyst.* 18, 2872–2886. doi: 10.1002/2016gc006774

Swenson, R. (1997). "Introduction to Tertiary tectonics and sedimentation in the Cook Inlet Basin," in *1997 Guide to the Geology of the Kenai Peninsula, Alaska, Anchorage, Alaska*, eds S. Karl, T. Ryherd, and N. Vaughn, (Anchorage, AK: Alaska Geological Society).

Terhune, P. J., Benowitz, J. A., Trop, J. M., O'Sullivan, P. B., Gillis, R. J., and Freymueller, J. T. (2019). Cenozoic tectono-thermal history of the southern Talkeetna Mountains, Alaska: insights into a potentially alternating convergent and transform plate margin. *Geosphere* 15, 1–38. doi: 10.1130/GES02008.1

Thorkelson, D. (1996). Subduction of diverging plates and the principles of slab window formation. *Tectonophysics* 255, 47–63. doi: 10.1016/0040-1951(95)00106-9

Trop, J. (2008). Latest cretaceous forearc basin development along an accretionary convergent margin: South-central Alaska. *Geol. Soc. Am. Bull.* 120, 207–224. doi: 10.1130/b26215.1

Trop, J., Hart, W., Snyder, D., and Idleman, B. (2012). Miocene basin development and volcanism along a strike-slip to flat-slab subduction transition: stratigraphy, geochemistry, and geochronology of the central Wrangell volcanic belt, Yakutat-North America collision zone. *Geosphere* 8, 805–834. doi: 10.1130/ges00762.1

Trop, J., and Ridgway, K. (2007). "Mesozoic and Cenozoic tectonic growth of southern Alaska: A sedimentary basin perspective," in *Tectonic Growth of a Collisional Continental Margin: Crustal Evolution of Southern Alaska*, eds K. Ridgway, J. Trop, J. Glen, and J. O'Neill, (Boulder, CO: Geological Society of America), 55–94. doi: 10.1130/2007.2431(04)

Trop, J., Ridgway, K., Manuszak, J., and Layer, P. (2002). Mesozoic sedimentary-basin development on the allochthonous wrangellia composite terrane, Wrangell Mountains basin, Alaska: a long-term record of terrane migration and arc construction. *Geol. Soc. Am. Bull.* 114, 693–717. doi: 10.1130/0016-76062002114<0693:Msbdot<2.0.Co;2

Trop, J. M., Ridgway, K. D., and Sweet, A. R. (2004). Stratigraphy, palynology, and provenance of the Colorado Creek basin, Alaska, USA: oligocene transpressional tectonics along the central Denali fault system. *Can. J. Earth Sci.* 41, 457–480. doi: 10.1139/e04-003

Trop, J., Szuch, D., Rioux, M., and Blodgett, R. (2005). Sedimentology and provenance of the upper Jurassic Naknek formation, Talkeetna Mountains, Alaska: bearings on the accretionary tectonic history of the Wrangellia composite terrane. *Geol. Soc. Am. Bull.* 117, 570–588. doi: 10.1130/b25575.1

Trop, J. M., Benowitz, J., Cole, R. B., and O'Sullivan, P. (2019). Cretaceous to Miocene magmatism, sedimentation, and exhumation within the Alaska Range suture zone: a polyphase reactivated terrane boundary. *Geosphere* 15, 1–36. doi: 10.1130/GES02014.1

Turner, D., and Smith, T. (1974). *Geochronology and generalized geology of the central Alaska Range, Clearwater Mountains, and northern Talkeetna Mountains*. Alaska Division of Geological and Geophysical Surveys Open-File Report 72.

Umhoefer, P. (1987). Northward translation of Baja British-Columbia along the late Cretaceous to Paleocene margin of western North-America. *Tectonics* 6, 377–394. doi: 10.1029/TC006i004p00377

Valentino, J., Spotila, J., Owen, L., and Buscher, J. (2016). Rock uplift at the transition from flat-slab to normal subduction: the Kenai Mountains, Southeast Alaska. *Tectonophysics* 671, 63–75. doi: 10.1016/j.tecto.2016.01.022

Weislogel, A., Graham, S., Chang, E., Wooden, J., Gehrels, G., and Yang, H. (2006). Detrital zircon provenance of the late triassic songpan-ganzi complex: sedimentary record of collision of the North and South China blocks. *Geology* 34, 97–100.

Wilson, F. H., Hults, C. P., Mull, C. G., and Karl, S. M. (2015). Geologic map of Alaska. *U.S. Geol. Surv. Sci. Invest. Map* 3340:196. doi: 10.3133/sim3340

Wolfe, J., and Tanai, T. (1980). The Miocene Seldovia Point flora from the Kenai Group, Alaska. *U.S. Geol. Surv. Prof. Pap.* 1105:52.

Worthington, L., Gulick, S., and Pavlis, G. (2008). "Identifying active structures in the kayak island and pamplona zones: implications for offshore tectonics of the Yakutat Microplate, Gulf of Alaska," in *Active Tectonics and Seismic Potential of Alaska*, eds J. Freymueller, P. Haeussler, R. Wesson, and G. Ekstrom, (Washington DC: American Geophysical Union), 257–268. doi: 10.1029/179gm14

Worthington, L., Van Avendonk, H., Gulick, S., Christeson, G., and Pavlis, T. (2012). Crustal structure of the yakutat terrane and the evolution of subduction and collision in southern Alaska. *J. Geophys. Res. Solid Earth* 117:B01102. doi: 10.1029/2011jb008493

Conflict of Interest Statement: The author declares that the research was conducted in the absence of any commercial or financial relationships that could be construed as a potential conflict of interest.